A&A 462, 1–6 (2007)
DOI: 10.1051/0004-6361:20066339

Astronomy & Astrophysics

Role of the He I and He II metastables in the resonance 2p $^2P°_{1/2,3/2}$ B III level population

S. Djeniže, A. Srećković, and S. Bukvić

Faculty of Physics, University of Belgrade, PO Box 368, Belgrade, Serbia
e-mail: steva@ff.bg.ac.yu

Received 4 September 2006 / Accepted 13 October 2006

ABSTRACT

Aims. The aim of this work is to present atomic processes which lead to an extra population of the 2p $^2P°_{1/2,3/2}$ B III resonance levels in helium plasma generating intense radiation in the B III 206.578 nm and 206.723 nm lines.
Methods. The line profiles were recorded using a step-by-step (7.3 pm) technique which provides monitoring of the line shapes continually during the plasma decay and gives the possibility to compare line shapes at various times in the same plasma.
Results. On the basis of the line intensity decays of the doubly ionized boron resonance spectral lines in laboratory nitrogen and helium plasmas, we have found the existence of a permanent energy transfer from He I and He II metastables to the 2p $^2P°_{1/2,3/2}$ B III resonance levels. The shapes of the mentioned lines are also observed. At electron temperatures of about 18 000 K and electron densities about 1.1×10^{23} m^{-3}, the Stark broadening was found as a main B III line broadening mechanism. The measured Stark widths (W) are compared with the Doppler width (W_D) and with the splitting in the hyperfine structure (Δ_{hfs}). Our measured W data are found to be much higher than results obtained by means of various theoretical approaches.
Conclusions. The He I and He II metastables over populate the B III resonance levels leading to populations higher than predicted by LTE model. Consequently, the emitted B III resonance lines are more intense than expected from LTE model. This fact can be of importance if B III resonance line intensities are used for abundance determination purposes in astrophysics. Similar behavior can be expected for some lines emitted by astrophysical interesting emitters: Al III, Si III, Sc III, Cr III, V III, Ti III, Fe III, Co III, Ni III, Ga III, Zr III, Y III, Nb III, In III, Sn III, Sb III, Au III, Pb III and Bi III in hot and dense helium plasmas.

Key words. plasmas – atomic data – atomic processes – line: profiles – radiation mechanisms: non-thermal

1. Introduction

The interest for astrophysics of the doubly ionized boron (B III) resonance spectral lines (206.578 nm and 206.723 nm) is increasing throughout recent years (Dessauges-Zavadsky et al. 2006). Boron abundances for seven main-sequence B-type stars are determined from HST (Hubble Space Telescope) and STIS (Space Telescope Imaging Spectrograph) spectroscopy around the B III 206.6 nm line (Mendel et al. 2006; Venn et al. 2002; Proffitt & Quigly 2001). The 206.578 nm B III resonance line has been obtained and analyzed, also, for two Small Magellanic Cloud (SMC) B-type stars (Brooks et al. 2002). Boron abundances provide a unique and critical test of stellar evolution models that include rotational mixing, since boron is destroyed in the surface layers of stars through shallow mixing long before other elements are mixed from the stellar interior through deep mixing (Mendel et al. 2006). Therefore, knowledge of the 2p $^2P°_{1/2,3/2}$ B III resonance level population processes and the mechanisms that create the B III resonance line shapes and positions are of great interest in astrophysics (Proffitt et al. 1999). In the plasmas with electron temperatures (T) about 20 000 K and electron densities (N) higher than 10^{21} m^{-3} the Doppler and Stark broadening (Griem 1964, 1974) are important in the formation of B III resonance lines shapes. Recognizable contribution to the line shape comes from the emitter itself, due to possible splitting (Δ_{hfs}) in the hyperfine structure (*hfs*). The hyperfine structure of the spectral line is caused by the interaction of the electron angular momentum (J) with the nuclear spin (I). The splitting of the spectral line depends on the nuclear magnetic dipole moment and the electric quadrupole moment (Schwartz 1955) and can range over wide wavelength interval. Also, the isotope effect can influence the distribution of the components in the Δ_{hfs}. Boron has two stable isotopes: 20% ^{10}B and 80% ^{11}B in natural stage with $I = 3$ and $I = 3/2$, respectively (Fuller 1976). Their *hfs* splittings are investigated by Proffitt et al. (1999) (and references therein). Therefore, combination of various plasma conditions, expressed through plasma parameters like: electron density, electron temperature and species densities are responsible (together with the exterior field strengths) for the line intensity, shape and line centre position (Griem 1974). The aim of this work is to present atomic processes which lead to an over population of the 2p $^2P°_{1/2,3/2}$ B III resonance levels in a helium plasma generating intense radiation at the B III 206.578 nm and 206.723 nm wavelengths. We have also obtained the shapes of these lines. The measured widths are compared with the Doppler width (W_D) and with the existing Stark widths (W) (Konjević et al. 2002) and splitting in the hyperfine structure (Δ_{hfs}).

2. Experiment

A modified version of the linear, low-pressure, arc (Djeniže et al. 2004a,b, 2005a,b, 2006a,b) has been used as the plasma source. A pulsed discharge was created in a Pyrex discharge tube of 5 mm inner diameter and plasma length of 14 cm. The tube had an end-on quartz window. Boron atoms are produced cause erosion of the Pyrex discharge tube's walls. In order to ensure high

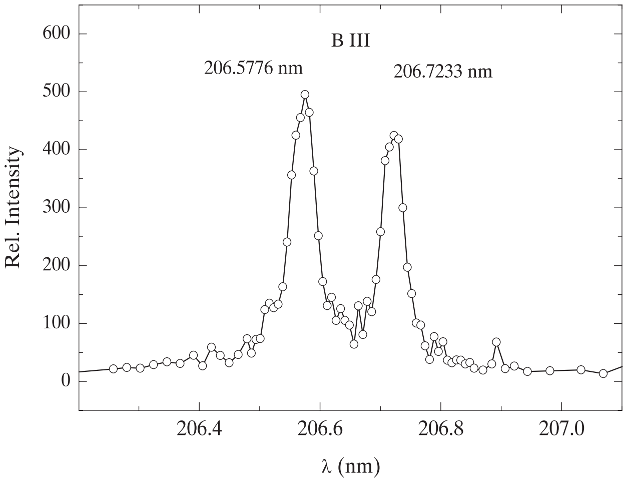

Fig. 1. The recorded B III resonance spectral line profiles using a step-by-step (7.3 pm) technique (five shots at the same position) in the helium plasma at 18 μs after the beginning of the discharge.

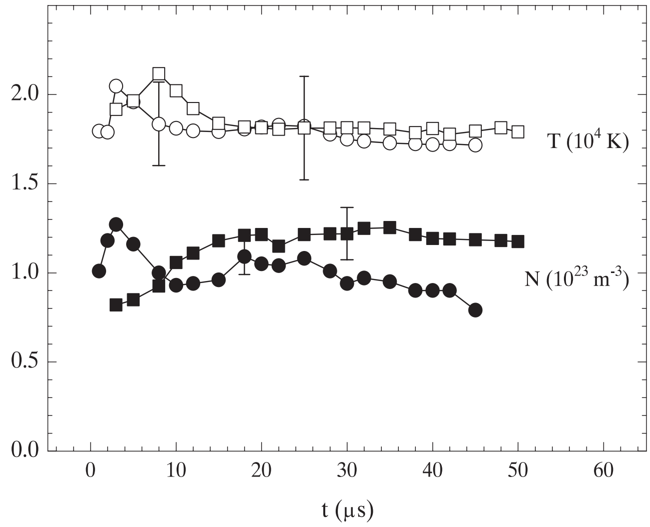

Fig. 2. Temporal evolutions of the electron temperature (T) and electron density (N) in the nitrogen (□, ■) and helium (○, ●) plasmas, respectively. The error bars represent estimated uncertainties (see the text).

evaporation of boron, the glass areas on the ends of the axial part of the discharge tube were enlarged. Nevertheless, the B III ion density obtained ensures an optically thin plasma for the investigated wavelengths. The absence of self-absorption was checked using a method described by Djeniže & Bukvić (2001). Applying this method we have found a value of 1.17 (±12%) for the line intensity ratio of the two B III lines which agrees with the value of 1.22 tabulated by NIST (2006). The working gas used was helium (90% He + 7% N + 3% O) and nitrogen (97% N +3% O) flowing at 1330 Pa and 133 Pa, respectively. A capacitor of 14 μF was charged up to 48 J bank energy. Plasma reproducibility was controlled by monitoring radiation originating from He I, He II, N II and N III lines, and the discharge current was controlled by using a Rogowski coil signal (it was found to be within ±4%). The spectroscopic observations of spectral lines were made end-on along the axis of the discharge tube. The line profiles were recorded using a step-by-step (7.3 pm) technique with the experimental set-up system described in our previous reports (Djeniže & Bukvić 2001). This technique provides monitoring of the total line intensity continually during the plasma decay and gives the possibility to compare line shapes at various stages of the same plasma. The photomultiplier signal was digitized using a digital scope interfaced to a computer. At each wavelength step five shots have been recorded and subsequently averaged. The recorded line profiles are shown in Fig. 1.

The plasma parameters were determined using standard diagnostic methods. The electron temperature was obtained using the relative intensity ratio method (Saha equation in Griem 1964, and in Rompe & Steenbeck 1967) between O II (395.436 nm and 397.326 nm) and O III (396.157 nm) spectral lines in the helium plasma with an estimated error of ±13% assuming the existence of the Local Thermodynamic Equilibrium (LTE). In the case of the nitrogen plasma the N II (463.054 nm) and N III (463.413 nm) spectral lines are used in the Saha equation. The estimated accuracy of T is ±16%. The necessary atomic data are taken from NIST (2006). The electron density decays were determined using known the Stark FWHM (Full-Width at Half of the Maximal intensity W) of the He II P_α (468.6 nm) spectral line within ±9% accuracy in the case of the helium plasma (Griem 1974), and using the convenient Stark widths of the 463.413 nm N III spectral line (Dimitrijević & Konjević 1981) within ±13% error. Temporal evolutions of the electron temperatures and electron densities are shown in Fig. 2.

The B III line profiles represent the convolutions of the Lorentzian Stark and Gaussian profiles caused by Doppler and instrumental broadening. For the electron density, electron temperature and density of the emitters in our experiment the Van der Waals and resonance broadenings were estimated to be smaller by more than one order of magnitude in comparison to the Stark, Doppler and instrumental broadening (Griem 1974). Therefore, we have used the Voigt function to fit our experimental line profiles. For the estimation of spectral line width a deconvolution procedure (Davies & Vaughan 1963) based on the least-squares algorithm is applied. Using this procedure we have associated uncertainties of ±16% for Stark widths. Contribution of the instrumental profile uncertainty is negligible.

3. Atomic processes

In order to determine the efficiency of the production of the B I and B III particles in the plasma, discharges in nitrogen and helium are used. In the same discharge tube and for the same detection conditions the B I (249.678 nm) and B III (206.578 nm) resonance line intensities have been monitored during the nitrogen and helium plasma decays. The B I line intensity maximum is approximately 3 times higher in nitrogen plasma (see Figs. 3 and 4). This means that the erosion of the discharge tube walls by electrons, N II, N III and N IV ions, in the nitrogen plasma, is about 3 times higher than those realized by electrons and He II ions in the helium plasma. Therefore, the density of the evaporated boron atoms is about 3 times higher in the nitrogen plasma. Temporal evolutions of the B III (206.578 nm) resonance line intensities in nitrogen and helium plasmas are presented in Figs. 3 and 4. The different shapes of these two curves is evident. In the nitrogen plasma it has one maximum at 15 μs after the beginning of the discharge (Fig. 3). In the helium plasma it has two maxima (Fig. 4). We found that intensity ratio of the successive maxima depends on the helium pressure. The first at 16 μs, is higher. The second is positioned about 32 μs after the beginning of the discharge. In order to explain the behavior of the B III line intensity decays, we have also monitored decays of spectral line

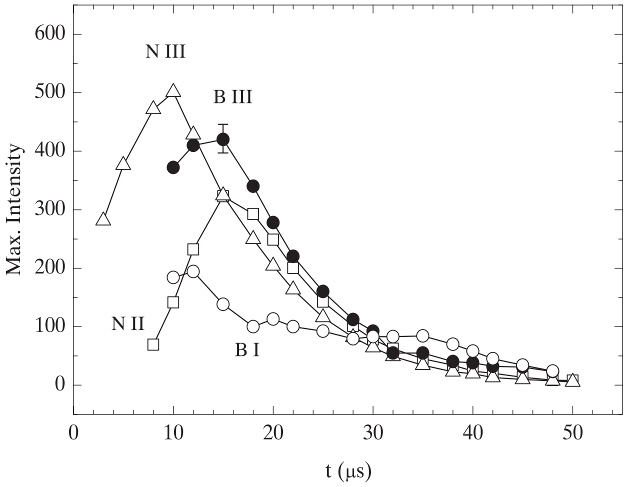

Fig. 3. Decays of the maximum intensities of the B I (249.6 nm) (○); B III (206.5 nm) (●); N II (463.0 nm) (□) and N III (463.4 nm) (△) spectral lines in the nitrogen plasma. The lines are recorded at the same discharge (p = 133 Pa, bank energy = 48 J) conditions. Values for N II and N III are 4 times reduced. Error bar represents ±6% uncertainties.

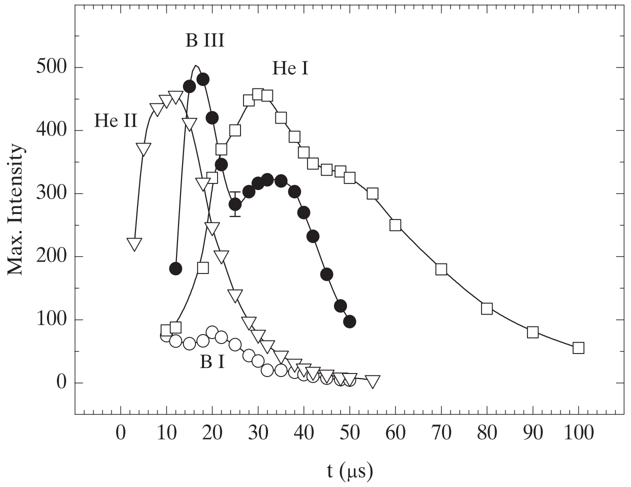

Fig. 4. Decays of the maximum intensities of the B I (249.6 nm) (○); B III (206.5 nm) (●); He I (388.9 nm) (□) and P_α He II (468.6 nm) (▽) spectral lines in the helium plasma. The lines are recorded at the same discharge (p = 1330 Pa, bank energy = 48 J) and detection conditions. Values for the P_α line are 13 times reduced. Error bar represents ±6% uncertainties.

intensities emitted by the main plasma components. The chosen spectral lines are: 463.073 nm N II, 463.416 nm N III, 388.865 nm He I and 468.6 nm He II (P_α-Paschen alpha). The corresponding intensity decays are also presented in Figs. 3 and 4. In the nitrogen plasma at T = 18 200 K and N = 1.2×10^{23} m^{-3}, the parent energy levels of the chosen N II (21.15 eV excitation energy) and N III (33.11 eV) transitions are populated under conditions provided by the LTE model (Rompe & Steenbeck 1967). The same also holds for the 2p $^2P°_{1/2,3/2}$ levels of the B III transition. It is evident, see Fig. 3, that the N II and N III line intensity decays have essentially the same form as the B III line intensity decay. Moreover, the N II and B III line intensities attain their maxima in the same moment (15 μs). The B III (206.5 nm)/B (249.6 nm) line intensity ratio maximum of 3.5, in the nitrogen plasma is realized at a 15 μs after the beginning of the discharge, exactly the moment when the B III line attains its maximum (Fig. 5). Within the experimental accuracy (±12%) this ratio decreases monotonously.

In the helium plasma (T = 18 000 K, $N = 1 \times 10^{23}$ m^{-3}) the B I (249.6 nm) resonance line intensity decay is similar to that in the nitrogen plasma (see Figs. 3 and 4). The B III (206.578 nm) resonance line intensity decay shows two maxima (Fig. 4), at 16 μs and 32 μs after the beginning of the discharge. The first maximum is realized practically simultaneously, within ±3 μs, of the P_α and B III maxima, in the case of the nitrogen plasma. The second maximum coincides with the 388.9 nm He I line maximum which is realized about 32 μs after the beginning of the discharge. This He I transition has a metastable 2s $^3S_1$ (19.82 eV, excitation energy) level as a final state and its intensity decay can give information about the density evolution of the helium metastables. One can conclude that the times of the P_α He II and 388.9 nm He I lines intensity maxima are also times when the He II and He I metastables have their maximum concentration. The coincidences mentioned clearly show an existing coupling between 2p $^2P°_{1/2,3/2}$ B III level population processes and the He I and He II metastables. The decay of the B III (206.5 nm) / B I (249.6 nm) intensity ratio (see Fig. 5) also confirms this claim. Although the density of evaporated boron atoms in helium is lower than in nitrogen, see Figs. 3 and 4, the B III / B I intensity ratio is significantly higher in the helium plasma. We

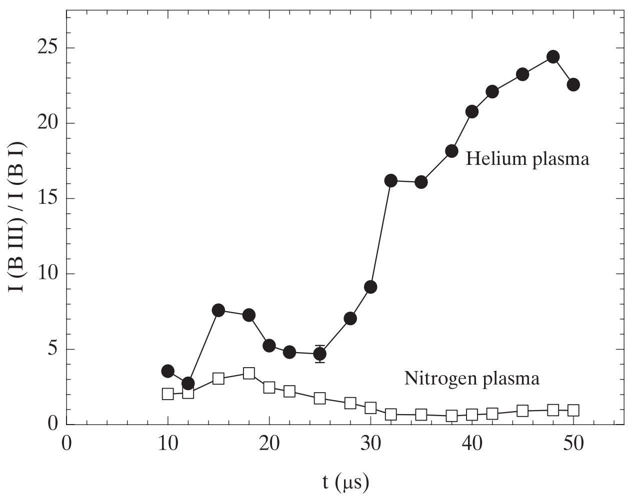

Fig. 5. Decays of the B III (206.5 nm) / B I (249.6 nm) maximum line intensity ratios in the nitrogen (□) and helium(●) plasmas. The B I and B III lines are recorded at the same discharge and detection conditions in the nitrogen and helium plasmas, respectively. Error bars represent ±12% uncertainties.

believe that the population of the 2p $^2P°_{1/2,3/2}$ B III levels in the helium plasma (at about 18 000 K electron temperature and $N = 10^{23}$ m^{-3}), additionally increases due to atomic processes in which the He*I (20.62 eV and 19.82 eV excitation energies) and He*II (40.813 eV) metastables play a main role (asterisk denotes metastable state). This extra population can be due to the Penning-effect (Kruithof & Penning 1937) through successive ionization processes:

$$\mathrm{He^*I(2s\ ^1S_0, 20.62\ eV) + BI(0.0\ eV) \rightarrow BII(12.26\ eV) + HeI(0.0\ eV) + e(0.06\ eV)} \quad (1)$$

$$\mathrm{He^*I(2s\ ^1S_0, 20.62\ eV) + BII(12.26\ eV) \rightarrow B\ III(6.0\ eV) + HeI(0.0\ eV) + e(1.74\ eV)} \quad (2)$$

$$\mathrm{He^*I(2s\ ^3S_1, 19.82\ eV) + BII(12.26\ eV) \rightarrow B\ III(6.0\ eV) + HeI(0.0\ eV) + e(0.94\ eV),} \quad (3)$$

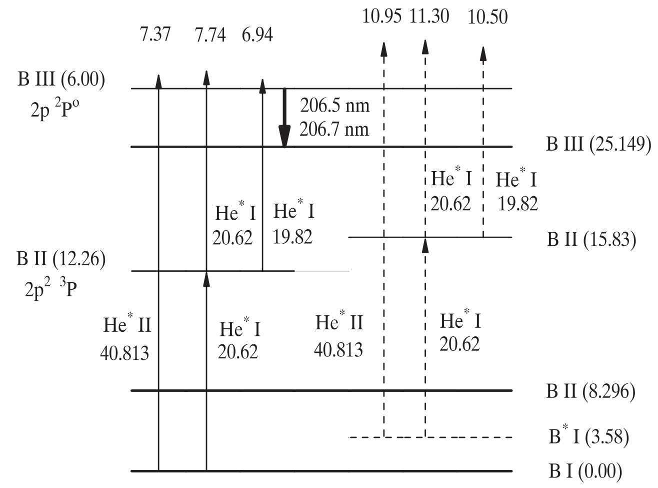

Fig. 6. Schematically presentation of the atomic processes, see Eqs. (1)–(4), leading to the 2p $^2P°_{1/2,3/2}$ B III resonance level population by He I and He II metastables. Dashed lines denote processes with B*I atoms. Asterisk denotes metastables. Atomic data are taken from NIST (2006). Numbers are expressed in eV units.

or due to the direct pumping from the B I ground state with participation of the He*II metastables:

$$\mathrm{He^*II}(2s\ ^2S_{1/2}, 40.813\ \mathrm{eV}) + \mathrm{BI}(0.0\ \mathrm{eV}) \rightarrow$$
$$\mathrm{B\ III}(2p\ ^2P°_{1/2,3/2}, 6.00\ \mathrm{eV}) + \mathrm{HeI}(0.0\ \mathrm{eV}) + e(1.37\ \mathrm{eV}). \quad (4)$$

The processes[1] described with Eqs. (1)–(4) are schematically presented in Fig. 6. It should be mentioned that similar processes starting from metastable level B*I (3.58 eV), instead from the boron ground state, are also energetically possible providing another channel for population of the 2p $^2P°_{1/2,3/2}$ B III resonance levels (see also Fig. 6). The role of the electron population processes is the same as in the nitrogen plasma. The helium ion metastables (with 40.813 eV excitation energy) can produce double ionization of boron atoms. The energy necessary for this process is: $E^I + E^{II} = 8.296\ \mathrm{eV} + 25.149\ \mathrm{eV} = 33.445\ \mathrm{eV}$, where E^I and E^{II} are the first and second ionization energies of boron (NIST 2006). The rest of the 40.813 eV–33.445 eV = 7.368 eV is enough for excitation of the 2p $^2P°_{1/2,3/2}$ B III resonance levels with $E^{III}_{\mathrm{exc}} = 6.00$ eV excitation energy. In similar way we can consider all these processes. Therefore, presence of the He*I and He*II metastables ensures permanent transfer of energy to B III resonance levels, leading to their populations being noticeable more than it is predicted by an LTE model. Consequently, the emitted B III resonance line intensities are much higher than is expected by the LTE model (see Figs. 3–5). This fact can be of importance if using B III resonance line intensities for abundance determination purposes in astrophysics in plasmas containing helium. The process described by Eq. (4) can be of great importance in hot and dense helium plasmas containing various emitters for which the sum $E^I + E^{II} + E^{III}_{\mathrm{exc}}$ is slightly less than 40.813 eV (Al III, Si III, Sc III, Cr III, V III, Ti III, Fe III, Co III, Ni III, Ga III, Zr III, Y III, Nb III, In III, Sn III, Sb III, Au III, Pb III and Bi III as examples of interest in astrophysics). If the effect of lowering the ionization energy (Unsöld 1948) is considerable, then the B II 12.691 eV energy level can also be directly populated by the Penning process from the boron ground state, Eq. (1), and finally contribute to the population of B III resonance level, Eq. (2). Namely, at an electron density of 10^{23} m^{-3} the calculated lowering of the first ionization energy is 0.324 eV (Drawin & Felenbok 1965), therefore, this process can also participate in the extra population of resonance B III level. As a result the corresponding spectral line (206.57 nm) is more intense than lines emitted by the helium itself, (see 388.9 nm He I line intensities in Fig. 4). The use of this spectral line intensity in various calculations based on an LTE assumption can produce a misleading result. As an example, we have calculated the electron temperature from the Saha equation applied to the 206.57 nm B III and 222.03 nm B II spectral lines (atomic data are taken from NIST and Kurucz). We have found $T = 49\,000$ K at 15 μs after the beginning of the discharge. This is about 3 times higher than if the lines satisfying LTE are employed, see Fig. 2.

[1] It is known that the He*I metastables (2s $^1S_0$ and 2s $^3S_1$) are of great importance for production of He II ions due to the Penning effect (Phelps & Molnar 1953; Pitchford et al. 1975). However, metastable levels of He II ions are only significantly populated in the case of higher electron temperatures and electron densities and so the last process (4) only applies to these conditions.

Table 1. Our measured B III Stark FWHM (W_m in pm) at a given T and N together with other experimental data (in various plasmas). W_D denotes the related Doppler width (Griem 1964). Δ_{hfs} represents the splitting in the hyperfine structure obtained by Proffitt et al. (1999). Transitions: 2s $^2S_{1/2}$–2p $^2P°_{3/2,1/2}$ and the *hfs*-free wavelengths are taken from NIST (2006).

λ (nm)	T (10^4 K)	N (10^{23} m^{-3})	W_m (pm)	Plasma	W_D (pm)	Δ_{hfs} (pm)	Reference
206.578	1.80	1.09	34.8 ± 5.6	He	6.1	5.1	This Work
	1.82	1.21	34.6 ± 5.6	N	6.1	5.1	This Work
	4.80	2.55	18.8	O	9.9	5.1	Srećković
	10.60	18.1	22.0	H	14.7	5.1	Glenzer
206.723	1.80	1.09	35.6 ± 5.7	He	6.1	5.3	This Work
	1.82	1.21	38.0 ± 6.1	N	6.1	5.3	This Work
	4.80	2.55	16.4	O	9.9	5.3	Srećković
	10.60	18.1	22.1	H	14.7	5.3	Glenzer

4. Line shape characteristics

Our measured Stark widths and other existing experimental width data are presented in Table 1. The Doppler widths (W_D) and the *hfs* splitting Δ_{hfs} are also presented. In order to compare existing experimental and theoretical data W of the B III resonance lines, their temperature dependence is presented in Fig. 7. In Dimitrijević & Konjević (1981), Stark widths of B III lines have been calculated within the semiempirical method (SE), the modified-semiempirical method (SEM), the simplified semiclassical method (G) and its modification (GM) for electrons as perturbers, only. GM and SEM values lie between G and SE values. Using the quantum mechanical close coupling method, Seaton (1988) calculated W and data calculated by Griem et al. (1997) agree with Seaton's predictions. They are about twice as small as the G, SEM, SE and GM values. In Dimitrijević & Sahal-Bréchot (1996), Stark widths of B III lines have been calculated using a semiclassical approach (DSB) for electrons, protons, and helium ions as perturbers. Only electron perturbers are important at densities of 10^{23} m^{-3}. All theoretical calculations predict very small W values, below 3 pm for T higher than 20 000 K. Only two experiments are devoted to measurements for the B III resonance lines. Srećković et al. (1993) measured W in a linear, low-pressure, pulsed arc operating in oxygen at a 48 000 K electron temperature. Glenzer & Kunze (1996) measured W at a 106 000 K electron temperature in hydrogen plasma created in a

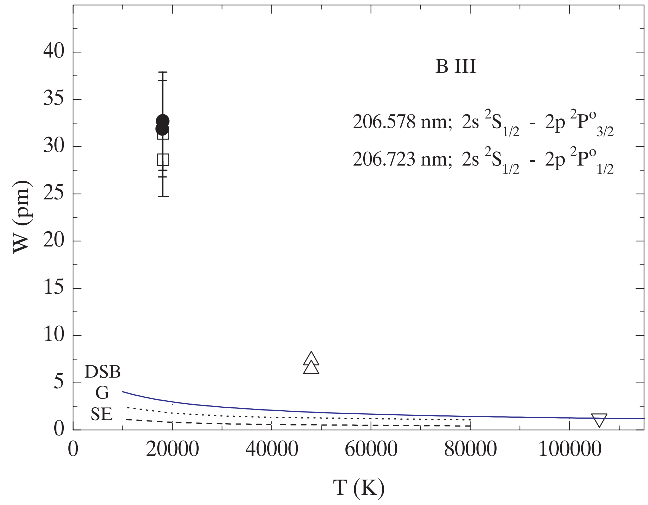

Fig. 7. Temperature dependence of the B III resonance lines Stark FWHM (W in pm) at 1×10^{23} m^{-3} electron density. Symbols SE and G denote calculated W values using various approximations in Dimitrijević & Konjević (1981) (see the text). Symbol DSB represents the recent (Dimitrijević & Sahal-Bréchot 1996) calculated W values using a semiclassical approach for electrons as perturbers. Symbols (•) and (□) represent our measured values in helium and nitrogen plasmas (within ±16% accuracy), respectively; while (Δ) and (∇) represent experimental data from Srećković et al. (1993) and Glenzer & Kunze (1996) obtained in oxygen and hydrogen plasma, respectively. Seaton's (1988) and Griem's (1997) data lie below the SE values.

linear-pinch. An agreement between DSB and Glenzer's (1996) experimental data was found. Explicit disagreement exists between Srećković's (1993) measurements and theoretical predictions. Our data are more than 10 times higher than those calculated by various approaches (see Fig. 7). On the other hand, our measured W for the 249.6 nm B I line is (4.8 ± 0.7) pm at 1.09×10^{23} m^{-3} electron density and is in agreement (within ±25%) with ones measured in Djeniže et al. (1992). Because of the observed absence of the self-absorption in the resonance B III lines, an explanation of this large disagreement is not easy. It possibly lies in the nature of the interaction between the electron core and the nucleus. Both the B III resonance spectral lines have four hyperfine components (Proffitt et al. 1999) with splitting 5.1 pm and 5.3 pm, respectively (see Table 1 and Fig. 8). It is evident that the theory does not include this. However, the Δ_{hfs} are up to 5 times higher than some calculated Stark widths at about 10^{23} m^{-3} electron density.

Starting from the assumption that the particular components in the B III *hfs* are all identically broadened we have constructed the estimated resulting line shape of the 206.57 nm B III line. Only the Stark broadening was used corresponding to the lowest W = 1 pm values (taken from Griem et al. 1997) for each component in the *hfs* (see Fig. 8).

5. Conclusion

On the basis of the line intensity decays of the doubly ionized boron resonance spectral lines in laboratory nitrogen and helium plasmas, we have found the existence of a permanent energy transfer from He I and He II metastables to the 2p $^2P°_{1/2,3/2}$ B III resonance levels. This leads to their population being much more than those predicted by the LTE model. This population can be produce by the Penning-effect through successive ionization processes or by direct population from the B I ground state by collisions with the He II metastables (recommended by us). These

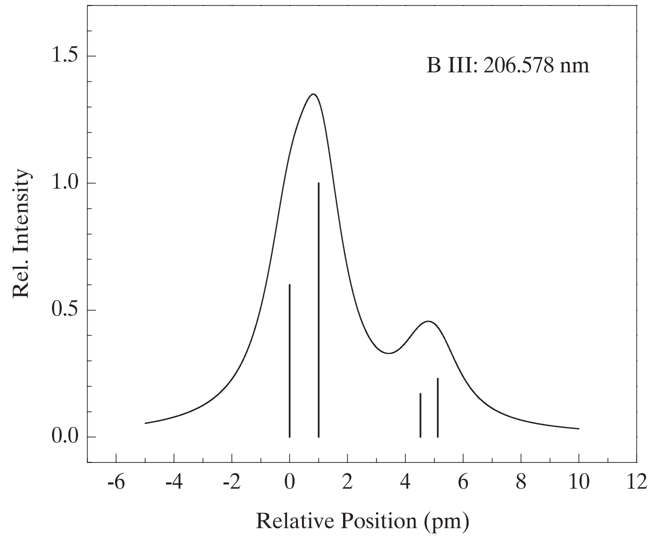

Fig. 8. The resulting profile of the 206.57 nm B III spectral line at 10^{23} m^{-3} electron density, constructed as a superposition of the particular Lorentz contribution for each component in the *hfs* pattern. The positions and intensities of the *hfs*-components are taken from Proffitt et al. (1999) taken into account the isotope contribution (1:4). The used theoretical Stark width was 1 pm (Griem et al. 1997).

population processes are always present in hot and dense helium plasmas. Consequently, the emitted B III resonance line intensities in helium plasma are much higher than those expected by the LTE model. This fact can be of importance when using B III resonance line intensities for abundance determination purposes in astrophysics. Similar behavior can be expected for some lines emitted by astrophysical interesting emitters: Al III, Si III, Sc III, Cr III, V III, Ti III, Fe III, Co III, Ni III, Ga III, Zr III, Y III, Nb III, In III, Sn III, Sb III, Au III, Pb III and Bi III in helium plasmas.

Our measured Stark FWHM are more than of 10 times higher than those calculated by various approaches. One explanation of this disagreement originates from the resulting line width being created by the contributions of the different components in the *hfs*.

Acknowledgements. This work is a part of the project "Determination of atomic parameters on the basis of spectral line profiles" supported by the Ministry of Science and Environmental Protection of the Republic of Serbia.

References

Brooks, A. M., Venn, K. A., Lambert, D. L., et al. 2002, ApJ, 573, 584
Davies, J. T., & Vaughan, J. M. 1963, ApJ, 137, 1302
Dessauges-Zavadsky, M., Prochaska, J. X., D'Odorico, S., Calura, F., & Matteucci, F. 2006, A&A, 445, 93
Dimitrijević, M. S., & Konjević, N. 1981, in Spectral Line Shapes, ed. B. Wende, (New York: W. de Gruyter, & Co), 521
Dimitrijević, M. S., & Sahal-Bréchot, S. 1996, A&AS, 119, 369
Djeniže, S., & Bukvić, S. 2001, A&A, 365, 252
Djeniže, S., Srećković, A., Labat. J., & Platiša, M. 1992, Phys. Scripta, 45, 320
Djeniže, S., Bukvić, S., & Srećković, A. 2004a, A&A, 425, 361
Djeniže, S., Bukvić, S., & Srećković, A. 2004b, ApJS, 151, 399
Djeniže, S., Srećković, A., & Bukvić, S. 2005a, Spectrochim. Acta B, 60, 1552
Djeniže, S., Srećković, A., & Bukvić, S. 2005b, Z. Naturforsch. A, 60a, 282
Djeniže, S., Bukvić, S., Srećković, A., & Nikolić, Z. 2006a, New Astron., 11, 257
Djeniže, S., Srećković, A., & Nikolić, Z. 2006b, J. Phys. B: At. Mol. Opt. Phys. 39, 3037
Drawin, H. W., & Felenbok, P. 1965, Data for Plasmas in Local Thermodynamic Equilibrium (Paris: Gauthier-Villars)

Fuller, G. H. 1976, J. Phys. Chem. Ref. Data, 5, 835
Glenzer, S., & Kunze, H.-J. 1996, Phys. Rev. A, 53, 1225
Griem, H. R. 1964, Plasma Spectroscopy (New York: McGraw Hill)
Griem, H. R. 1974, Spectral Line Broadening by Plasmas (New York: Acad. Press)
Griem, H. R., Ralchenko, Y. V., & Bray, I. 1997, Phys. Rev. E, 56, 7186
Konjević, N., Lesage, A., Fuhr, J. R., & Wiese, W. L. 2002, J. Phys. Chem. Ref. Data, 31, 819
Kruithof, A. A., & Penning, F. M. 1937, Physica, 4, 430
Kurucz, R. L., Atomic Spectral Line Database from CD-ROM 23
Mendel, J. T., Venn, K. A., Proffitt, C. R., Brooks, A. M., & Lambert, D. A. 2006, ApJ, 640, 1039
NIST 2006, Atomic Spectra Database Lines (wavelength order) http://www.physics.nist.gov
Phelps, A. V., & Molnar, J. P. 1953, Phys. Rev., 89, 1202
Pitchford, L. C., Taylor, K. N., & Collins, C. B. 1975, J. Phys. B: At. Mol., 8, 142
Proffitt, C. R., Jönsson P., Litzén, U., Pickering, J. C., & Wahlgren, G.M. 1999, ApJ, 516, 342
Proffitt, C. R., & Quigly, M. F. 2001, ApJ, 548, 429
Rompe, R., & Steenbeck, M. 1967, Ergebnisse der Plasmaphysik und der Gaselektronik, Band I (Berlin: Akademie Verlag)
Schwartz, C. 1955, Phys. Rev., 97, 380
Seaton, M. J. 1988, J. Phys. B: At. Mol. 21, 3033
Srećković, A., Djeniže, S., & Platiša, M. 1993, in Proc. of the 16th SPIG, ed. M. Milosavljević (Institute of Nuclear Sciences "Vinča", Belgrad), 201
Unsöld, A. 1948, Z. Astrophys., 24, 355
Venn, K. A., Brooks, A. M., Lambert, D. L., et al. 2002, ApJ, 565, 571